Cell Host & Microbe
Article

HIV-1 Buds and Accumulates in "Nonacidic" Endosomes of Macrophages

Mabel Jouve,[1] Nathalie Sol-Foulon,[2] Sarah Watson,[1] Olivier Schwartz,[2] and Philippe Benaroch[1,*]
[1] Institut Curie, INSERM U653, 26 rue d'Ulm 75248 Paris Cedex 05, France
[2] CNRS URA1930, Institut Pasteur, 25-28 rue Dr Roux 75724 Paris Cedex 15, France
*Correspondence: benaroch@curie.fr
DOI 10.1016/j.chom.2007.06.011

SUMMARY

Macrophages represent viral reservoirs in HIV-1-infected patients and accumulate viral particles within an endosomal compartment where they remain infectious for long periods of time. To determine how HIV-1 survives in endocytic compartments that become highly acidic and proteolytic and to study the nature of these virus-containing compartments, we carried out an ultrastructural study on HIV-1-infected primary macrophages. The endosomal compartments contain newly formed virions rather than internalized ones. In contrast to endocytic compartments free of viral proteins within the same infected cells, the virus containing compartments do not acidify. The lack of acidification is associated with an inability to recruit the proton pump vacuolar ATPase into the viral assembly compartment. This may prevent its fusion with lysosomes, since acidification is required for the maturation of endosomes. Thus, HIV-1 has developed a strategy for survival within infected macrophages involving prevention of acidification within a devoted endocytic virus assembly compartment.

INTRODUCTION

Assembly of HIV requires a spatio-temporal coordination to gather the various viral and cellular components that constitute the viral particles to specific location(s) of infected cells. Numerous studies performed in lymphocytes have identified the plasma membrane as the main platform for assembly, budding, and pinching of viral particles (Morita and Sundquist, 2004). Only a few studies have been performed in primary macrophages where viral assembly appears to follow essentially the same steps but at a different location. In these cells, early ultra structural studies have shown that HIV-1 viral particles accumulate in intracellular vacuoles (Gartner et al., 1986; Gendelman et al., 1988; Orenstein et al., 1988). These vacuoles contain high levels of class II molecules of the Major Histocompatibility Complex (MHC II) and present the characteristics of multivesicular bodies (MVBs) or MIIC (Pelchen-Matthews et al., 2003; Raposo et al., 2002). MIIC are endosomal compartments where MHC II acquire their peptide cargo. In macrophages, the assembly of HIV-1 in MVBs explains the particular content of the membrane in which the viral particles are wrapped, which notably contains high amounts of MHC II, cholesterol, and some tetraspanins (Chertova et al., 2006; Kramer et al., 2005; Nydegger et al., 2006; Pelchen-Matthews et al., 2003).

Ultrastructural studies suggested that assembly of HIV-1 particles occurs at the limiting membrane of these MVBs/MIIC in the same way as that by which internal vesicles of MVBs are formed (Raposo et al., 2002). Supporting this interpretation, the cellular machinery, called ESCRT, which is involved in the biogenesis of MVBs and operates at their limiting membrane, is required for HIV-1 assembly (see review Morita and Sundquist, 2004). This occurs through the precursor Pr55Gag, which recruits the ESCRT machinery by interacting with TSG101 and Alix/AIP1. In noninfected T cells and macrophages, TSG101, as well as Alix/AIP1, is distributed throughout the whole endocytic pathway (Welsch et al., 2006). This pathway is highly dynamic, especially in macrophages, which are specialized in phagocytosis and degradation of external material. The relationship between the dynamics of the endocytic pathway and the compartment in which HIV-1 particles get assembled in infected macrophages remains largely unknown.

Virus-containing MVBs can fuse with the plasma membrane and thereby release their contents into the extracellular medium (Raposo et al., 2002), which potentially contributes to the spreading of the infection. Indeed, these intracellular viral particles were elegantly shown to be infectious as they can be affinity purified with antibodies specific for membrane proteins like MHC II and CD63 (Kramer et al., 2005; Pelchen-Matthews et al., 2003). Therefore, an important open question is to understand how HIV-1 particles can survive in the endocytic pathway, which a priori is rather hostile to the virions. Intracellular HIV-1 particles in macrophages can be recovered after cell disruption and are able to persist and to retain infectivity for weeks (Sharova et al., 2005). Importantly, viral particle exposure to acidic pH leads to a complete loss of their infectivity (Ongradi et al., 1990). MVBs are acidic prelysosomal organelles, whose fate is to fuse with lysosomes thereby leading to the degradation of the material present in the MVB lumen.

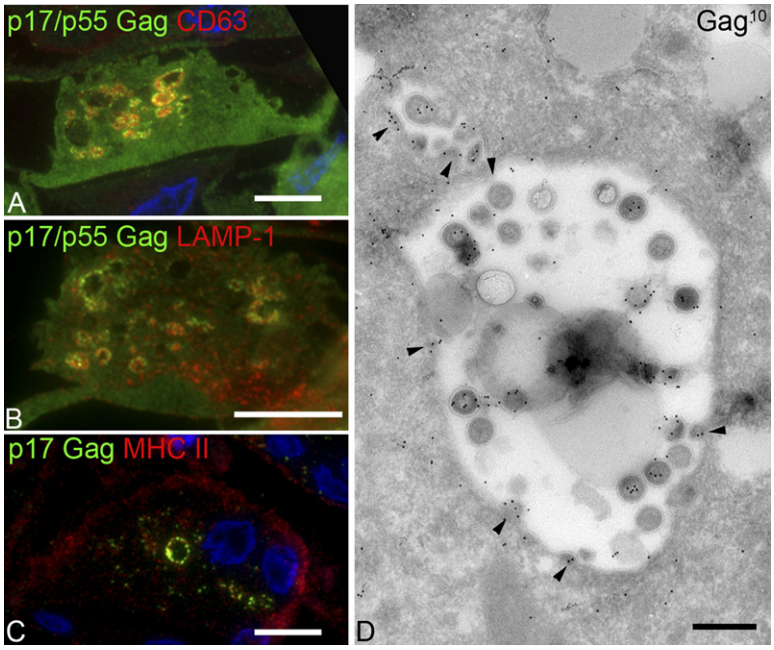

Figure 1. HIV-1 Virions Bud and Accumulate in an Intracellular Compartment of Infected Primary Macrophages

Semithin (A–C) and ultrathin (D) cryosections of MDM infected with HIV-1 NLAD8 for 15 days were prepared. Semithin sections were double-labeled for Gag and for CD63, LAMP-1, or MHC II. In (A) and (B) antibodies were specific for p17 and the parental protein (referred to as p17/p55), which is present everywhere in the cells, whereas in (C) antibodies were specific only for p17. Gag staining with both types of antibodies was undetectable in noninfected cells (data not shown). Nuclei were stained with DAPI and are shown in blue on the merged images, (see also Figure S1 for single labeling of the same fields). A substantial colocalization of Gag with CD63, LAMP-1 and MHC II is observed in intracellular granules. Scale bars, 5 μm.

(D) Ultrathin cryosections were labeled with antibodies specific for p17/p55 and Protein A coupled to gold particles of 10 nm diameter (PAG 10). Budding virions can be seen at different stages of completion (see arrowheads), including one still attached by a thin stick to the limiting membrane. Scale bars, 200 nm.

The endocytic pathway is full of active proteases able to degrade viral particles. In dendritic cells, which possess a phago-lysosomal system less aggressive than that of macrophages (Savina et al., 2006), internalization of HIV-1 particles through DC-SIGN leads to the rapid inactivation of the virions (Moris et al., 2004). Thus, newly synthesized viral particles accumulating in endosomal compartments of macrophages should be rapidly inactivated and degraded. Macrophages exposed to HIV-1 internalize viral particles and target them for degradation in lysosomes (Marechal et al., 2001). On the contrary, in infected macrophages, endogenously produced viral particles can survive and remain infectious for six weeks (Sharova et al., 2005). In addition, despite a slower rate of production of virions in macrophages as compared to T cells, infected perivascular macrophages and microglia represent important viral reservoirs in vivo (Gonzalez-Scarano and Martin-Garcia, 2005).

To determine how HIV-1 can survive in endocytic compartments and to study the nature of the virus-containing compartments, we carried out an ultrastructural study on HIV-1-infected primary macrophages. Their endosomes were characterized by monitoring the morphology, the presence of endosomal/lysosomal markers as well as the presence of viral proteins and particles, the kinetics of accessibility to endocytic tracers, and the acidity of these compartments. Our data indicate that newly synthesized virions are stored in a specific compartment that is not correctly acidified probably as the result of the lack of recruitment of the V-ATPase. In contrast, other endocytic compartments present in the same infected macrophages are correctly acidified and represent the final destination of endocytosed viral particles. By preventing correct acidification of its assembly and storage compartment, HIV-1 may preserve its viability.

RESULTS

HIV-1 Particles Assemble at the Limiting Membrane of Compartments Containing Endocytic Markers

Monocytes were prepared from human peripheral blood by MACS sorting using anti-CD14 beads. The purity of the monocyte-enriched fraction was generally superior to 97% as judged by FACS analysis at day 3 of culture on the basis of CD14 and MHC II expression (data not shown). Monocytes were infected with NLAD8 or YU2 macrophage tropic strains and cultured in the presence of M-CSF. As expected, chronic infections were established and cultures were maintained for up to 3 weeks, but generally used at 2 weeks. The time course of HIV-1 production was monitored by measuring p24Gag in cell supernatants (data not shown). Percentages of Gag+ cells were also determined by flow cytometry on permeabilized cells. Cultures with concentration of p24 superior to 100 ng/ml in the supernatant and containing more than 10% of Gag+ cells were fixed and processed for immuno-EM. From these blocks, semithin sections of monocytes-derived macrophages (MDM) infected with the NLAD8 strain were first analyzed by immunofluorescence. As expected, usage of antibodies able to recognize p17, as well as the precursor Pr55Gag, generated a diffuse pattern where large intracellular compartments appeared brighter (Figures 1A and 1B, and Figure S1 in the Supplemental Data available with this article online). In contrast, usage of the p17Gag specific antibodies, gave rise to a discrete vesicular staining (Figure 1C and Figure S1).

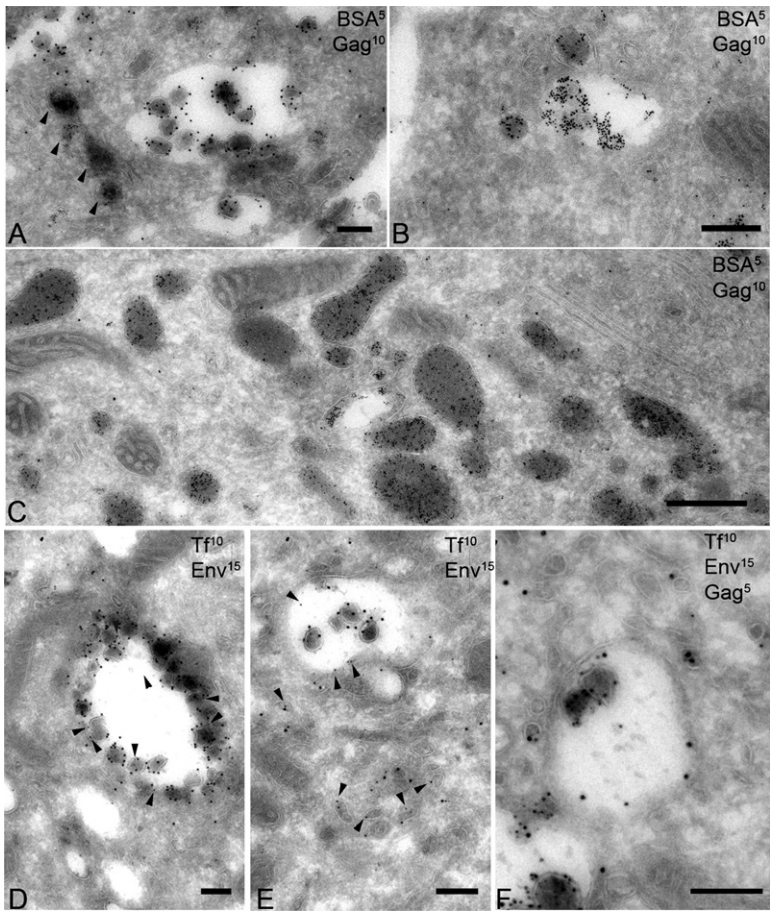

Figure 2. Dynamic Access of Endocytic Tracers to the Virus-Containing Compartment

MDM infected with HIV-1 NLAD8 for 15 days were exposed either to BSA-gold (5 nm) for 2 hr at 37°C (A–C) or to Tf-Alexa488 for 30 min at 37°C (D and E). Cells were prepared for cryosectioning and immunogold-labeled for Gag (polyconal anti-p17/p55) with PAG10 (A–C) or for Env with PAG15, and for Tf-Alexa488 with anti-Alexa-488 antibodies and PAG10 (D and E). In (F), triple labeling for Gag, Env, and Tf was performed. In (A), the virus-containing compartments have hardly any BSA-gold particle as compared to Gag-negative MVBs (B) and lysosomes (C), where BSA-gold particles are very numerous. In (A), arrowheads point to lysosomes containing BSA-gold particles near a virion-containing compartment. (D and E) Tf is indicated with arrowheads in the virus-containing compartments. The compartment in (E) possesses associated tubules containing Tf. (F) The virus-containing compartment is labeled for the 3 markers indicating that HIV particles positive for Gag and Env are in a compartment accessible to internalized Tf. Scale bars, 200 nm.

Overall, Gag staining was found in large intracellular compartments containing CD63, MHC II molecules and low levels of LAMP-1 (Figure 1 and Figure S1).

Ultrathin cryosections prepared from the same blocks were labeled for Pr55Gag and analyzed by EM (Figure 1D). We observed large intracellular compartments containing in their lumen viral particles with a typical immature morphology (electron dense at the periphery and electron lucent at the core). We also observed budding profiles at the limiting membrane of such compartments. These buds appeared to be at various stages of the process (Figure 1D, see arrowheads and for instance, at the bottom a virion just beginning to bud, and at the top, a virion still attached by a thin membrane ready to pinch off). Gag staining was clearly restricted to a subpopulation of intracellular compartments, often containing viral particles. These compartments sometimes contained lipids (see in the center of the main compartment in Figure 1D) in agreement with a recent report suggesting that HIV-1-infected macrophages accumulate substantial amounts of lipids due to a Nef-mediated mechanism leading to impaired cholesterol efflux (Mujawar et al., 2006). Similar results were obtained with the YU2 strain of HIV-1 (data not shown). We concluded that our preparations of infected MDM contain intracellular compartments positive for Gag, CD63, MHC II, and LAMP-1. There, newly synthesized virions get assembled and stored. Moreover, HIV-1-infected MDM clearly possess different populations of endosomes, some of which free of viral proteins.

Access of Dynamic Tracers to the Endocytic Pathway in HIV-1-Infected Macrophages

To characterize further these assembly compartments and their relationship with the dynamics of the endocytic pathway, infected MDM were exposed for 2 hr at 37°C to BSA-gold particles (5 nm) as an endocytic tracer. Cells were then washed, fixed, and processed for immuno-EM. We observed that the virus-containing compartments had strikingly lower levels of BSA-gold (Figure 2A) than those present in neighboring MVBs free of Gag-specific labeling (Figure 2B) and in lysosomes within the same cells (Figure 2A, see arrowheads, and 2C). The difference was roughly 38-fold less BSA-gold in virus-containing compartments compared to Gag-negative MVBs (mean values: 52 ± 34 versus 1975 ± 72 BSA-gold particles/μm^2). Thus, whereas the endosomal/lysosomal continuum appeared intact in HIV-1-infected MDM, the virus-containing compartments were hardly accessible to BSA-gold, suggesting that they were away from the main endocytic route.

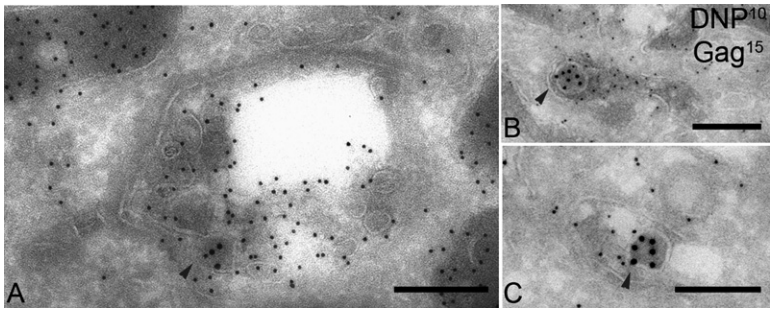

Figure 3. Fate of Internalized HIV-1 Particles in MDM

(A to C) MDM were exposed to a high MOI of HIV-1 NLAD8 particles for 2 hr at 37°C, and then chased in the presence of DAMP for 30 min. Cells were then fixed and processed for immuno-EM. Ultrathin cryosections were double-labeled for DNP with PAG10, and for p24/p55 Gag with PAG15. Three examples of compartments containing a viral particle positive for Gag (see arrowhead) and substantial DNP-labeling are presented. Therefore, internalized viral particles access acidic compartments. Scale bars, 200 nm.

We next investigated whether these assembly compartments intersect the recycling pathway. HIV-1-infected MDM were allowed to internalize Transferrin (Tf) coupled to Alexa488 for 30 min at 37°C, to fill sorting and recycling endosomes. Double immuno-gold labeling of infected MDM revealed that the compartments containing Env-positive viral particles were accessible to Tf-Alexa488 (Figures 2D and 2E). Finally, Gag and Env-positive particles were observed in compartments labeled for Tf-Alexa488 (Figure 2F).

Taken together, these results indicate that the viral particles assemble and reside in a compartment that possesses unusual characteristics: it intersects the recycling route of the Tf, but is hardly accessible to endocytic tracers like BSA-gold, and possesses markers of late endosomes/MVBs.

Lack of Acidification of the Virus-Containing Compartment

Acidification occurs gradually within the endocytic pathway. To examine the acidity of the compartments containing viral particles, we had to distinguish these compartments from other endosomes, free of viral components. Therefore we turned to the weak base 3-(2,4-dinitroanilino)-3′ amino-N-methyldipropylamine (DAMP), which is lipophilic and can diffuse across membranes. It accumulates in acidic structures and remains there after aldehyde fixation where it can be detected with dinitrophenol (DNP)-specific antibodies (Anderson et al., 1984; Orci et al., 1986). First, the specificity of the DAMP technique was evaluated at the ultrastructural level on MDM possessing an alkalinized endosomal system due to Concanamycin B (ConB) exposure. ConB is a potent inhibitor of the vacuolar ATPase (V-ATPase) (Yilla et al., 1993), the proton pump responsible for the acidification of the whole vacuolar system. Noninfected MDM exposed or not to ConB, and then to DAMP, were fixed and processed for immuno-EM. The anti-DNP labeling was intense in untreated MDM, in MVBs (Figure S2B), and especially in electron dense compartments, which in all likelihood were lysosomes (Figure S2A). MDM exposed overnight to ConB contained more MVBs, which were larger (Figure S2C), as previously observed in human B cells (Benaroch et al., 1995). Moreover, these MVBs contained very low amounts of protons as detected by the DAMP technique. This illustrated the validity of this technique to evaluate at the ultrastructural level the concentration of protons in various intracellular compartments.

Second, we had to distinguish newly synthesized viruses accumulated in MVBs from eventual endocytosed viral particles, which could originate from neighboring cells. We therefore exposed MDM to high MOI of viral preparations for 2 hr at 37°C and chased in the presence of DAMP for 30 min. Cells were then fixed and processed for cryosectioning. Ultrathin sections labeled for Pr55Gag and DNP revealed low amounts of viral particles only present in acidic structures, (i.e., positive for DNP) (Figure 3). This indicates that, in MDM, endocytosed/phagocytosed viruses are targeted to acidic compartments of the endocytic system. These results are in agreement with a previous study showing that HIV-1 entry in macrophages mainly occurs by macropinonocytosis and that inhibition of macropinocytosis leads to a strong reduction of HIV entry and replication (Marechal et al., 2001).

Next, MDM were exposed to DAMP, washed and prepared for cryosectioning and immuno-labeling. Analysis of semithin sections of infected MDM stained by immunofluorescence allowed an overview of the distribution of DAMP relative to other proteins of interest. DAMP accumulated primarily in compartments containing LAMP-1, but strikingly not in p55Gag-positive compartments (Figures 4A–4C).

Next, cryosections of infected MDM exposed to DAMP were triple immunogold-labeled and analyzed by immuno-EM. We observed that lysosomes (Figure 4D) and Gag-negative MVBs (Figure 4E) were heavily labeled with the anti-DNP mAb, indicating their strong acidity. In sharp contrast, compartments containing Gag-positive particles exhibited a much lower DNP labeling (Figures 4F–4H). Thus, on the same sections, lysosomes highly positive for DNP can be seen next to DNP-low to negative compartments containing viral particles (see a general view on Figure S3A). These results were confirmed by immunofluorescence after exposure of infected MDM to the Lysostracker to probe acidic compartments. Confocal microscopy revealed that Gag-positive compartments were not stained for Lysotracker (Figure S3B).

A quantitative analysis of the density of the DNP labeling in the various compartments was carried out (see Figure 5 and Table 1). Looking at the noninfected cells, the density of the DNP labeling was clearly shifted from MVBs to

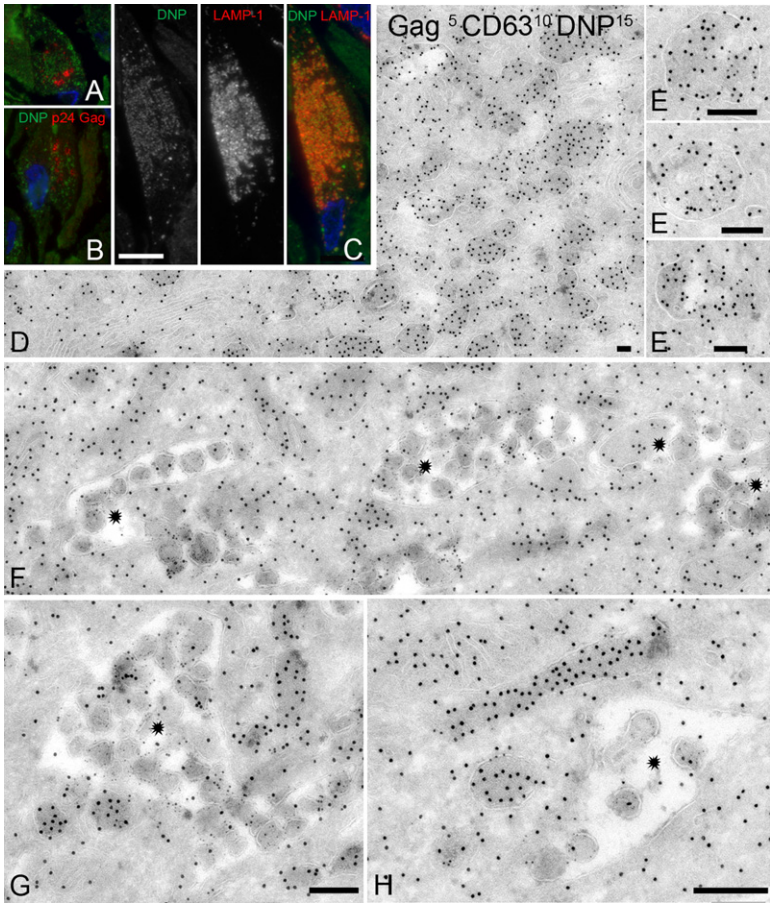

Figure 4. HIV-1 Particles Accumulate in Nonacidic Compartments

MDM infected with HIV-1 NLAD8 for 15 days were exposed to DAMP for 30 min and prepared for cryosectioning.

(A–C) Semithin sections were stained for the indicated markers. DAPI was used to stain nuclei and appears in blue on the merged images. Scale bars, 5 μm. In (C), single color and merged images are presented to allow better estimation of the codistribution of the markers. Lysosomes are not evenly distributed among cryosections explaining their apparent absence on some cellular profiles. DNP does not colocalize with mature Gag and, thus, with HIV-1 particles, whereas it does with LAMP-1.

(D–H) Ultrathin cryosections were triple labeled for DNP with PAG15, for CD63 with PAG10, and for p17/p55 Gag with PAG5. (D) Overview of the extended endolysosomal system in infected MDM, where the richness of the DNP labeling can be appreciated. (E) Three examples of Gag-negative MVBs exhibiting a DNP rich labeling. (F–H) Three examples of virus-containing compartments are shown (see the stars). They present a DNP labeling rather poor as compared to neighboring lysosomes. Scale bars, 200 nm.

lysosomes to higher values, as expected, as measured by the density of gold particles per μm^2 (Figure 5A; Table 1). Upon HIV-1 infection, Gag-negative MVBs from HIV-1-infected cells were denser and, thus, more acidic than their counterpart in control cells. In contrast, the acidity of the lysosomes remained unchanged (Figures 5A and 5B; Table 1). Strikingly, in infected cells, the density of gold particles present in the virus-containing compartments was reduced 13.4 times as compared to MVBs free of viral particles (Figure 5B, Table 1). These data clearly establish that HIV-1-containing compartments are far less acidic than Gag-negative MVBs or than lysosomes.

Morphological Analysis of the Effects of HIV-1 Infection on the Endocytic Pathway of Primary Macrophages

Having characterized the virus-containing compartments in infected MDM, we examined the other endocytic compartments using DAMP immunolabeling. Infected cells were identified by the presence of viral particles in intracellular compartments and by Gag labeling. The general morphology of the lysosomes was comparable in both types of cells (compare Figure 4D and Figure S2A). However, quantification of their surface revealed that the lysosomes were slightly smaller in HIV-1-infected cells as compared to uninfected MDM (Figures 5C and 5D; Table 1). This might reflect the fact that MVBs containing viral particles do not fuse with lysosomes.

The frequency of MVBs in uninfected cells was rather low. Examination of numerous cryosections was necessary to compare MVBs in infected or uninfected MDM. In both situations, MVBs free of viral proteins were usually spherical compartments of 300 to 500 nm diameter containing internal vesicles (Figure 4E). Their size distribution in MDM was not affected by the HIV-1 infection (Figures 5C and 5D; Table 1). In contrast, the virus-containing compartments exhibited a very heterogeneous size distribution (see Figure 5D and examples in Figures 1D, 4F–4H; Figure S3A).

We concluded that HIV-1 infection in MDM does not alter the whole endo-lysosomal system but rather induces the proliferation of an intracellular compartment, which is highly heterogeneous in size and which contains viral particles.

The pH Control of the Virus-Containing Compartment Is Independent of NOX2 Activity

The vacuolar pH mainly depends on the coordinated activity of two enzymes: the NADPH oxidase NOX2 and the V-ATPase. NOX2 mediates the production of reactive

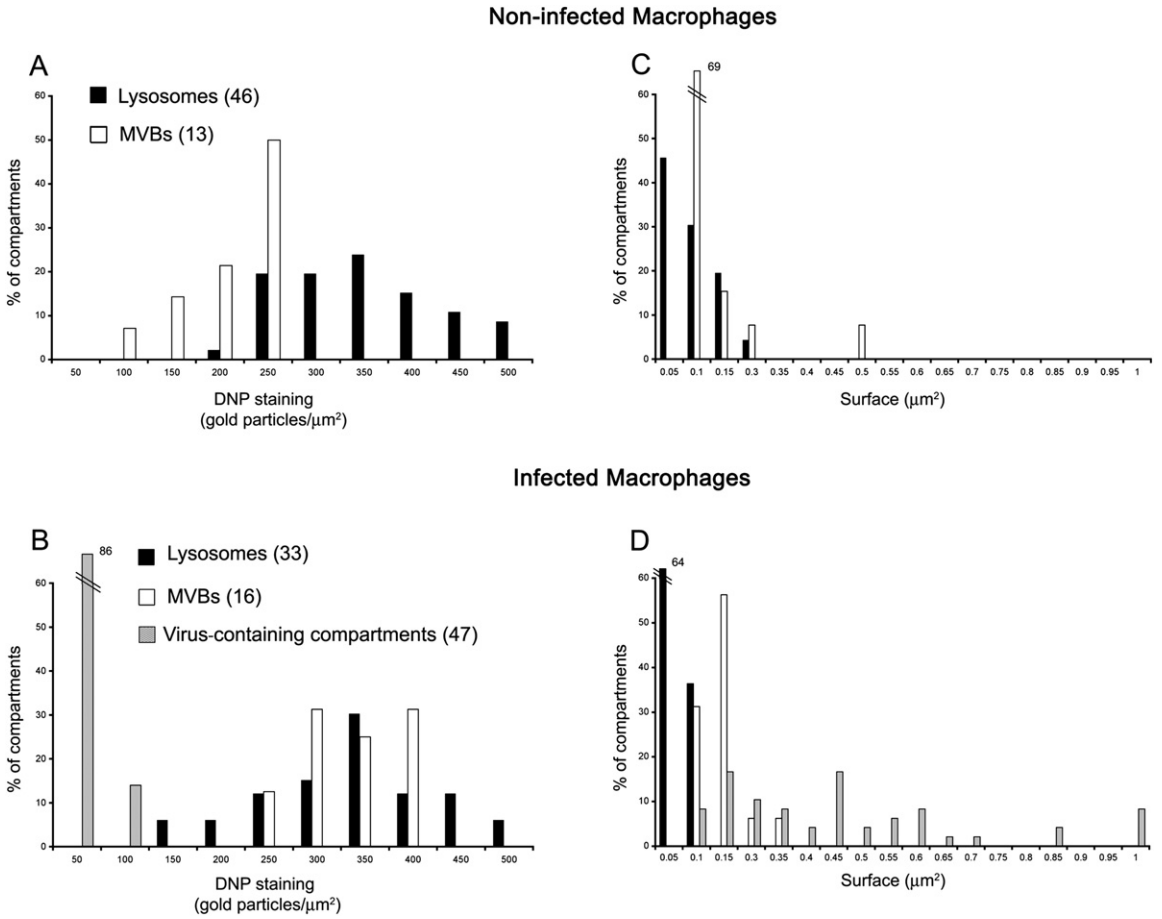

Figure 5. Quantitative Analysis of DNP-Labeled Cryosections

Cryosections of uninfected or HIV-1 NLAD8-infected MDM, labeled for DNP and Gag as in Figure 4, were used to perform a quantitative analysis of the DNP staining.

(A and B) Distribution of the density of the DNP staining among the various compartments is shown for uninfected MDM (A) and for infected MDM (B). Results are expressed as percentages of compartments possessing a given density of DNP-specific gold particles/μm^2. For each type of compartment, the sum of these percentages is equal to 100%. Lysosomes were defined as electron-dense compartments possessing a rich DNP labeling. MVBs were identified by morphological criteria: the presence of internal vesicles and also the absence of Gag staining (in [B]). In contrast, virus-containing compartments were defined on the basis of the presence of Gag-positive particles. The numbers between brackets indicate the number of given compartments used for the quantification.

(C and D) The distribution of the surface of the endocytic compartments is shown for uninfected (C) and for infected MDM (D). Results are expressed as percentages of compartments possessing a given surface. For each type of compartment, the sum of these percentages is equal to 100%.

oxygen species in the organellar lumen, resulting in proton consumption and alkalinization. The potential involvement of NOX 2 in the control of the pH of the virus-containing compartments was tested by two means. First, we estimated the consequences of the inhibition of NOX2 activity on the pH of the virus-containing compartments, on the production of virus, and on their infectivity. Infected MDM were exposed to 5 µM DPI for 30 min, an inhibitor of NOX enzymes. The efficiency of the DPI exposure on NOX activity was checked using the nitroblue tetrazolium (NBT) assay (Oliveira et al., 2003). NOX activity in MDM was markedly inhibited after DPI exposure (Figures S4A and S4B). Infected MDM exposed to DPI and then to DAMP were prepared for immuno-EM analysis. Figure S4C shows that the anti-DNP antibody very efficiently labeled lysosomal structures (mean value: 292 gold/μm^2) but generated a very poor labeling of the virus-containing compartment (mean value: 26 gold/μm^2), as observed in untreated cells (see Figures 4 and 5). Therefore, DPI exposure did not modify the concentration of protons in the virus-containing compartment.

Second, we used a cell line deficient for NOX2. The PLB 985X-CGD cell line was obtained by disruption of the gp91phox subunit of NOX2, by homologous recombination in the PLB-985 human myeloid cell line (Zhen et al., 1993). Both cell lines were infected with HIV-1 NL-4.3 at two different MOI. After 48 hr, viral production and infectivity were similar in both cell lines (Figure S5C). Viral production was also similar when NOX positive and negative cells were exposed to a single cycle HIV-1 virus

Table 1. Statistical Analysis of the DNP Labeling in Endocytic Compartments

Compartments	Lysosomes		Gag-Negative MVBs		Gag-Positive MVBs
Cells	CTRL	HIV	CTRL	HIV	HIV
Density (gold/μm^2)	324.6 ± 73.7	357.8 ± 93.1	218.5 ± 83.2	315.7 ± 52.3	23.5 ± 18.4
p value	0.09		*1.6 10^{-3}**		*1.7 10^{-13}**
Surface (μm^2)	0.071 ± 0.041	0.046 ± 0.016	0.118 ± 0.089	0.120 ± 0.044	0.394 ± 0.396
p value	*5.9 10^{-4}**		0.94		*4.2 10^{-5}**

Quantification of the DNP labeling on cryosections analyzed by immuno-EM was performed as explained in Figure 5. The same data were used here to calculate mean values ± their SEM. Density is expressed as the number of DNP-specific gold particles per μm^2 of the indicated compartments. CRTL means noninfected control MDM. These data indicate that the pH of lysosomes in HIV-1-infected and control MDM is comparable, whereas the pH of Gag negative MVBs is significantly more acidic in HIV-1-infected cells as compared to control cells. Conversely, the surface of lysosomes is significantly smaller in HIV-1-infected cells, while the surface of Gag-negative MVBs remains similar after HIV-1 infection.
* p values were calculated using the Student's t test. They are presented in italics when inferior to 0.05.

(NL-4.3ΔEnv pseudotyped with VSV-G, data not shown). Moreover, the examination by immuno-EM of the mutated cells, revealed intracellular compartments containing viral particles positive for Gag with very low concentration of protons as determined with the DAMP assay (Figure S5B). Other compartments were Gag-negative and exhibited an intense DNP staining (Figure S5A).

Taken together, these data indicate that NOX 2 activity is not involved in neutralizing the pH of the virus-containing compartment in infected MDM.

Lack of V-ATPase Recruitment to the Virus-Containing Compartments

Having ruled out the involvement of NOX activity, we turned to the V-ATPase. This enzyme is responsible for the acidification of the whole vacuolar system. The V-ATPase consumes ATP to translocate protons into the lumen of the compartments in which it is inserted, leading to its acidification. Thus, we then tested whether V-ATPase was correctly recruited at the limiting membrane of the virus-containing compartments. The intracellular distribution of the V-ATPase was analyzed by immunofluorescence on semithin sections of infected MDM. An antibody specific for the 16 kD V-ATPase subunit of the V0 complex generated an intense staining of numerous intracellular compartments heterogeneous in size. Strikingly, the V-ATPase staining extensively colocalized with LAMP-1 but failed to label Gag-positive compartments (Figure 6). Next, we tested the effect of the V-ATPase inhibitor ConB on viral production. HIV-1-infected MDM exposed to 20 nM ConB for 24 or 40 hr produced similar or even higher amounts of p24 in their supernatant, supporting the idea that the V-ATPase is not involved in the HIV assembly process.

These results show that in MDM, the viral assembly takes place into a particular compartment of the endocytic pathway from which the V-ATPase seems excluded. Other endocytic compartments present in the same cells, but free of viral proteins, still recruit the enzymatic complex and therefore are correctly acidified.

DISCUSSION

Our immuno-EM analysis of primary MDM infected by HIV-1 reveals that newly synthesized virions are produced and stored in a compartment with unusual characteristics. It contains specific markers of late endosomes such as CD63, MHC II, and low amounts of LAMP-1, in agreement with previous studies (Pelchen-Matthews et al., 2003; Raposo et al., 2002). This compartment is heterogeneous in size and contains various numbers of viral particles. HIV-infected MDM internalize BSA-gold, which efficiently reaches their extended lysosomal system, indicating that the endolysosomal system overall functions correctly. In contrast, internalized BSA-gold hardly reaches the virus-containing compartment. Similar results were obtained using IgG-gold in a seminal study on infected macrophages (Orenstein et al., 1988). Moreover, we show that the acidification of the compartment is impaired probably due to the inefficient recruitment of a functional proton pump, the V-ATPase. Thus, the compartment is not a bona fide late endosome/MVB as previously thought (Nydegger et al., 2003; Pelchen-Matthews et al., 2003; Raposo et al., 2002; Ryzhova et al., 2006; Sharova et al., 2005). It is somehow away from the main endocytic route and appears to be connected to the recycling pathway, as shown by its accessibility to internalized Tf. Its content in late endocytic markers CD63, LAMP-1, CD81, and CD82 appears to differ from the one observed in late endocytic compartments of uninfected cells (Deneka et al., 2007; Kramer et al., 2005; Pelchen-Matthews et al., 2003). Therefore, HIV-1 appears to specifically affect the cellular protein composition of the compartment to devote it to viral assembly and storage.

We present here evidence establishing that intracellular virions observed in our preparations of HIV-1-infected macrophages are not endocytosed particles, as recently suggested (Jouvenet et al., 2006), but represent, in their vast majority, newly synthesized virions. Figure 1D is demonstrative as it shows viral particles at various stages of budding at the limiting membrane of the compartment. The viral particles we observed at the ultrastructural level

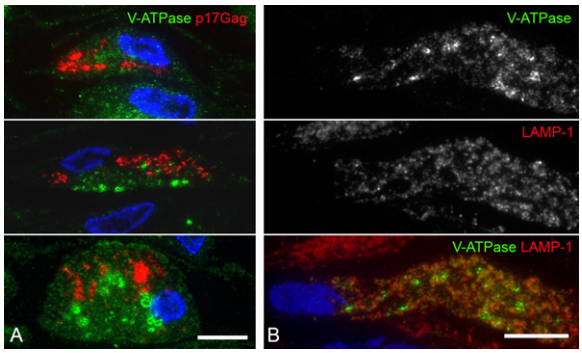

Figure 6. The V-ATPase is not Efficiently Recruited at the Limiting Membrane of HIV-1 Assembly Compartments

Semithin cryosections of MDM infected with HIV-1 NLAD8 for 15 days were double-labeled for the C subunit of the V-ATPase V0 complex (revealed by Cy3-labeled secondary antibodies) and for p17 Gag (A) or for LAMP-1 (B) (revealed by Alexa488-labeled secondary antibodies). DAPI staining was performed to visualize the nucleus (in blue). In (A), merged images representative of three independent experiments are presented. In (B), single color and merge images are presented to allow estimation of the extent of the codistribution of both markers. The V-ATPase does not colocalize with Gag whereas it partially does with LAMP-1. Scale bar, 5 μm.

are immature virions, as judged by their electron lucent material at the core and electron dense material at the periphery. Mature virions can occasionally be seen and are recognizable due to their central electron dense material (see arrowheads, Figure S3). Among our numerous EM observations of infected macrophages, we never observed budding profiles at the plasma membrane, contrary to infected Jurkat T cells (data not shown). Moreover, the HIV-1 strains we used in the present study express Vpu. Recently, this accessory protein was shown to promote virus release but also to inhibit virus uptake by endocytosis (Harila et al., 2006; Neil et al., 2006). We also performed control experiments by exposing MDM to viral preparations of high MOI for 2 hr at 37°C that were chased for 30 min in the presence of DAMP. Analysis of such preparations revealed that virions were only present in acidic endosomal structures (Figure 3). Therefore, when MDM internalize virions, the later are targeted to degradative acidic compartments. These results are in agreement with a previous study showing that, shortly after exposure of macrophages to HIV-1, most virions are found in macropinosomes and subsequently degraded (Marechal et al., 2001). Taken together, our results strongly suggest that in our preparations of HIV-1-infected MDM, viral assembly takes place in an intracellular compartment of endocytic origin and not at the plasma membrane. Thus, this compartment is referred to as the viral assembly compartment.

During submission of this manuscript, two studies were published indicating that, in HIV-infected macrophages, viral particles can be found in new intracellular structures connected to the plasma membrane by narrow channels (Deneka et al., 2007; Welsch et al., 2007). Our findings regarding the lack of recruitment of the V-ATPase, as well as the access of Tf, are compatible with this new structure. It is worth noting that both studies were based on the usage of ruthenium red, a dye supposed to be membrane impermeant and, thus, to only stain membranes accessible to the external milieu. However, ruthenium red can get access to internal structures depending on the lipids and the glycoproteins encountered by the dye during fixation (Hayat, 2000; Luft, 1971). It is also possible that some of the viral compartments accessible to ruthenium red have initiated a process of exocytosis of their viral contents and are thus connected to the plasma membrane. To further document the accessibility of the HIV-containing compartment to the extracellular milieu, we stained HIV-infected macrophages with ruthenium red. Approximately, 20% of the virus-containing compartments were positive for this dye (Figure S6), whereas all of them exhibit a lack of acidification (Figures 4 and 5). Our observations are in agreement with a recent report showing that a good proportion of virus-containing compartments are not stained by ruthenium red (Welsch et al., 2007). Therefore, these substantial numbers of virus-containing compartments inaccessible to ruthenium red clearly represent intracellular compartments of endocytic origin.

The main finding of this study is that the viral assembly compartment, which is also the place where virions are stored, is not correctly acidified. In contrast, other endocytic compartments, including lysosomes and MVBs present in the same infected macrophages, are correctly acidified. Considering that the pH of the nucleus is neutral (pH 7.0), quantification of the DAMP labeling can be used to estimate pH values for intracellular compartments (Orci et al., 1986). From our data, the estimation of the pH of the viral assembly compartment is pH 6.8. This pH value is far from the acidic pH known to inactivate the virus (Garcia et al., 2005; Ongradi et al., 1990), and should contribute to the survival of stored particles.

Acidification of the whole vacuolar system in macrophages mainly relies on the activity of the V-ATPase. This multicomponent enzyme is made of two large complexes, named V0 and V1, each composed of several subunits (Nishi and Forgac, 2002). V0 is inserted into membranes and is responsible for pumping protons in the lumen of the compartments. V1 contains the ATPase activity and is first assembled in the cytosol and then recruited onto V0. Following the C subunit of the membrane-associated V0 complex, we show that this subunit is not recruited to the viral assembly compartment whereas it is clearly associated to LAMP-1 positive compartments. This suggests that the V-ATPase is inefficiently or partially recruited to the membrane of the viral assembly compartment and is responsible for their pH. Moreover, inhibition of the V-ATPase in HIV-infected MDM did not affect the viral production, confirming that the V-ATPase activity does not influence the viral assembly process in MDM.

Inhibition of the activity of the V-ATPase in uninfected cells somehow mimics the effect of HIV-1 infection: it blocks endosomal trafficking (Clague et al., 1994; van Deurs et al., 1996), it neutralizes the pH of the endocytic

compartments, and it induces their swelling and the accumulation of intralumenal vesicles (Benaroch et al., 1995). Moreover, it prevents their fusion with lysosomes (van Weert et al., 1995), which potentially enhances their targeting to the plasma membrane and the release of exosomes (G. Raposo, personal communication). One of the subunits of the V-ATPase functions as a pH sensor. Upon acidification of the endosomal lumen, it allows the recruitment of molecular coats necessary for endosomal trafficking on the cytosolic side of the endosomes (Hurtado-Lorenzo et al., 2006). Therefore, it is likely that preventing the recruitment of a functional V-ATPase to the viral assembly compartment is advantageous to the virus. It may prevent the fusion of these compartments with lysosomes, leading with time to the accumulation of numerous viral assembly compartments, which can be observed in infected macrophages. These compartments may then proceed to homotypic fusion and lead to the very large compartments that can be sometimes observed in HIV-infected macrophages. Interestingly, homotypic vacuole fusion in yeast depends on the V-ATPase (Ungermann et al., 1999). Moreover, a subunit of the V0 complex is required for the fusion of MVBs with the plasma membrane and for the release of exosomes in the *C. elegans* model (Liegeois et al., 2006). It remains to be determined whether incomplete recruitment of the V-ATPase to the viral assembly compartment could impede the proton pump activity and promote homotypic fusion and virus release by fusion with the plasma membrane.

A new mode of regulation of acidification has been reported in dendritic cells: phagosomes recruit the NOX2 enzyme, which results in proton consumption in the phagosome lumen (Savina et al., 2006). However, our results indicate that NOX2 activity is not involved in the lack of acidification of the viral assembly compartment of infected macrophages.

Several viral gene products could be involved in the impairment of the recruitment of the V-ATPase. Among them, Nef appears a likely candidate since it can interact with the V-ATPase (Lu et al., 1998), induce MVBs accumulation, and affect the endocytic pathway (Sanfridson et al., 1997; Stumptner-Cuvelette et al., 2003). However, in MDM, the pH of the viral assembly compartment is identical for wild-type and ΔNef virus, as determined by the DAMP technique (Figure S7). This is in agreement with a previous report showing that Nef was not required for the survival of intracellular viral particles in macrophages (Sharova et al., 2005). In the same study, Vpu, which is involved in viral particle release, was shown to be dispensable for survival of intracellular viral particles. Experiments to identify the viral gene product(s) involved in the control of the acidification of the virus-containing compartments are currently performed.

Other pathogens have evolved similar strategies to survive in macrophages. One of the best-studied examples is the intracellular bacteria *Mycobacterium tuberculosis*. After getting phagocytosed, it inhibits the fusion of the phagosome with lysosomes. This inhibition results from different strategies, including the impairment in the delivery of several subunits of the V-ATPase to the phagosome through a PI3 kinase-dependent pathway (Vergne et al., 2004). The same mechanism also prevents acidic proteases to reach the bacterial phagosome. This compartment fails to be acidified and thus becomes a "friendly" environment for the bacteria, accessible to internalized Tf, containing low levels of LAMP-1 and unable to fuse with lysosomes, (see Vergne et al., 2004). Thus, in macrophages, it shares several important features with the HIV-1 assembly compartment, as reported in the present study. These two pathogens have also physiopathological relationships. *M. tuberculosis* is the most common opportunistic infection in AIDS (De Cock et al., 1992). It is a sentinel disease for HIV, often indicative of potentially undiagnosed AIDS cases. The extent of the similarities of the mechanisms evolved by both pathogens in macrophages remains to be determined as well as the eventual physiological consequences.

Several lines of evidence support a pivotal role of monocytes/macrophages in viral persistence. Indeed, infectious virus can be recovered from blood monocytes of patients receiving HAART, whereas no viral particle is detected in their blood (Lambotte et al., 2004). In the brain, macrophages and microglia are the most productively HIV-infected cells. The ultrastructural analysis of brain biopsy specimen from patients with AIDS encephalopathy revealed viral budding profiles at the limiting membrane of intracellular compartments, which accumulate virions (Orenstein et al., 1988). Thus, the viral assembly process we document in the present study with in vitro infected monocytes probably takes place in vivo.

EXPERIMENTAL PROCEDURES

Reagents and Antibodies

DAMP and Tranferrin-AlexaFluor 488 were from Molecular Probes. Diphenylene iodinium (DPI), an NADPH-oxidase inhibitor, was from Calbiochem. Secondary reagents used for immunofluorescence on semithin sections were Alexa488-conjugated goat anti-rabbit Ig (from Molecular Probes), Cy3-conjugated donkey anti-mouse Ig or anti-rabbit Ig, and Cy3-conjugated streptavidine and were purchased from Jackson Immuno Research Laboratories.

The following antibodies were used in single, double, or triple immunolabeling experiments: rabbit polyclonal antibodies specific for p17 as well as p55 (NIH AIDS reagents 4811 from P. Spearman); a mAb specific for the matrix (p17), obtained from the National Institute for Biological Standards and Control (NIBSC) centralized facility for AIDS reagents (ARP342, from R.B. Ferns and R.S. Tedder); a biotinylated mAb specific for p24 as well as p55 (NIBSC ARP 454, from R.B. Ferns and R.S. Tedder); human polyclonal antibodies anti-Gp120 (NIBSC EVA 3064, from H. Katinger); an anti-CD63 mAb from PeliCluster; an anti-LAMP-1 mAb from PharMingen; rabbit antibodies specific for the V-ATPase V0 C subunit kindly provided by M. Skinner; rabbit polyclonal antibodies specific for HLA-DR kindly provided by H.L. Ploegh; and rabbit polyclonal antibodies anti-Alexa488 and anti-DNP from Molecular Probes.

Cell Culture and Infection

The production and use of HIV-1 (NL4.3 and NLAD8 strains) have been described (Marechal et al., 2001). Primary CD14+ cells (purity superior to 95%, less than 0.8% of CD3+ cells contamination) were exposed to the NLAD8 virus (viral input 100 ng p24/ml/5.10^6 cells) for 2h30, washed with PBS and cultured for 15 or 21 days in the presence of

M-CSF (25 ng/ml). For HIV-1 replication experiments, PLB and PLBΔNox cells were exposed to the NL4.3 virus (viral input 10–20 or 100–200 ng p24/ml/ 10^6 cells) for 2.5 hr, washed with PBS, and cultured in 24 well plates in duplicates. Viral release was monitored by measuring HIV-1 Gag p24 production in supernatants by ELISA (Perkin-Elmer Life Science). Single-cycle infections of P4C5 cells with viruses produced from PLB and PLBΔNox were performed as described (Marechal et al., 2001). Infectivity was measured 36 hr after viral exposure.

Dynamic Uptakes

Tranferrin Uptake

Cells were washed with serum-free medium and starved 1 hr before incubation with Tf-Alexa488 (60 μg/ml) (Molecular Probes) for 30 min at 37°C. Cells were rinsed twice with ice-cold medium and processed for cryotomy.

Uptake of DAMP or of BSA-Gold

Cells were washed with serum-free medium and incubated either with BSA-gold for 2 hr at 37°C or/and with DAMP (30 μM) for 30 min at 37°C. Cells were washed with ice-cold medium and fixed before processing for cryotomy. When indicated, cells were pretreated for 30 min with DPI (5 μM) immediately before DAMP incubation.

Microscopy

Cells were fixed and processed for cryomicrotomy as described previously (Raposo et al., 2002). Protein A coupled to gold particles of 5, 10, or 15 nm diameter, and BSA coupled to gold particles of 5 nm diameter was purchased from G. Posthuma (University Medical Center, Utrecht, The Netherlands). EM chemicals were from Electron Microscopy Sciences (Pennsylvania). Sections were observed and photographed under a Philips CM120 electron microscope (FEI, Eindoven, The Netherlands). Digital acquisitions were made with a numeric camera Keen View and analyzed using the Item software (Soft Imaging System, Munster, Germany). The profiles presented are representative of at least 2 to 4 independent experiments. Semithin sections were stained with fluorescent secondary antibodies, washed, and mounted in moviol. Images were captured using a 64× oil immersion objective on a Leica DMRB microscope using a Nikon ACT-1 version 2.00 software.

Supplemental Data

The Supplemental Data include seven supplemental figures and can be found with this article online at http://www.cellhostandmicrobe.com/cgi/content/full/2/2/85/DC1/.

ACKNOWLEDGMENTS

M.J. was supported by a fellowship, and P.B. by a grant from "Ensemble contre le SIDA." This study was supported by a grant from "Agence Nationale de Recherche contre le SIDA" to P.B. We thank B. Asjo for her support at the beginning of the study; F.-X. Gobert for his help in setting up the figures; J. el Benna for assistance with the NBT assay; M.C. Dinauer for the gift of the PLB cell lines; and S. Amigorena, G. Raposo, and A. Savina for discussion.

Received: February 27, 2007
Revised: May 11, 2007
Accepted: June 29, 2007
Published: August 15, 2007

REFERENCES

Anderson, R.G., Falck, J.R., Goldstein, J.L., and Brown, M.S. (1984). Visualization of acidic organelles in intact cells by electron microscopy. Proc. Natl. Acad. Sci. USA *81*, 4838–4842.

Benaroch, P., Yilla, M., Raposo, G., Ito, K., Miwa, K., Geuze, H.J., and Ploegh, H.L. (1995). How MHC class II molecules reach the endocytic pathway. EMBO J. *14*, 37–49.

Chertova, E., Chertov, O., Coren, L.V., Roser, J.D., Trubey, C.M., Bess, J.W., Jr., Sowder, R.C., 2nd, Barsov, E., Hood, B.L., Fisher, R.J., et al. (2006). Proteomic and biochemical analysis of purified human immunodeficiency virus type 1 produced from infected monocyte-derived macrophages. J. Virol. *80*, 9039–9052.

Clague, M.J., Urbe, S., Aniento, F., and Gruenberg, J. (1994). Vacuolar ATPase activity is required for endosomal carrier vesicle formation. J. Biol. Chem. *269*, 21–24.

De Cock, K.M., Soro, B., Coulibaly, I.M., and Lucas, S.B. (1992). Tuberculosis and HIV infection in sub-Saharan Africa. JAMA *268*, 1581–1587.

Deneka, M., Pelchen-Matthews, A., Byland, R., Ruiz-Mateos, E., and Marsh, M. (2007). In macrophages, HIV-1 assembles into an intracellular plasma membrane domain containing the tetraspanins CD81, CD9, and CD53. J. Cell Biol. *177*, 329–341.

Garcia, E., Pion, M., Pelchen-Matthews, A., Collinson, L., Arrighi, J.F., Blot, G., Leuba, F., Escola, J.M., Demaurex, N., Marsh, M., and Piguet, V. (2005). HIV-1 trafficking to the dendritic cell-T-cell infectious synapse uses a pathway of tetraspanin sorting to the immunological synapse. Traffic *6*, 488–501.

Gartner, S., Markovits, P., Markovitz, D.M., Kaplan, M.H., Gallo, R.C., and Popovic, M. (1986). The role of mononuclear phagocytes in HTLV-III/LAV infection. Science *233*, 215–219.

Gendelman, H.E., Orenstein, J.M., Martin, M.A., Ferrua, C., Mitra, R., Phipps, T., Wahl, L.A., Lane, H.C., Fauci, A.S., and Burke, D.S. (1988). Efficient isolation and propagation of human immunodeficiency virus on recombinant colony-stimulating factor 1-treated monocytes. J. Exp. Med. *167*, 1428–1441.

Gonzalez-Scarano, F., and Martin-Garcia, J. (2005). The neuropathogenesis of AIDS. Nat. Rev. Immunol. *5*, 69–81.

Harila, K., Prior, I., Sjoberg, M., Salminen, A., Hinkula, J., and Suomalainen, M. (2006). Vpu and Tsg101 regulate intracellular targeting of the human immunodeficiency virus type 1 core protein precursor Pr55gag. J. Virol. *80*, 3765–3772.

Hayat, M.A. (2000). Principles and Techniques of Electron Microscopy: Biological Applications, Fourth Edition (Cambridge, UK: Cambridge University Press).

Hurtado-Lorenzo, A., Skinner, M., El Annan, J., Futai, M., Sun-Wada, G.H., Bourgoin, S., Casanova, J., Wildeman, A., Bechoua, S., Ausiello, D.A., et al. (2006). V-ATPase interacts with ARNO and Arf6 in early endosomes and regulates the protein degradative pathway. Nat. Cell Biol. *8*, 124–136.

Jouvenet, N., Neil, S.J., Bess, C., Johnson, M.C., Virgen, C.A., Simon, S.M., and Bieniasz, P.D. (2006). Plasma Membrane Is the Site of Productive HIV-1 Particle Assembly. PLoS Biol. *4*, e435. 10.1371/journal.pbio.0040435.

Kramer, B., Pelchen-Matthews, A., Deneka, M., Garcia, E., Piguet, V., and Marsh, M. (2005). HIV interaction with endosomes in macrophages and dendritic cells. Blood Cells Mol. Dis. *35*, 136–142.

Lambotte, O., Chaix, M.L., Gubler, B., Nasreddine, N., Wallon, C., Goujard, C., Rouzioux, C., Taoufik, Y., and Delfraissy, J.F. (2004). The lymphocyte HIV reservoir in patients on long-term HAART is a memory of virus evolution. AIDS *18*, 1147–1158.

Liegeois, S., Benedetto, A., Garnier, J.M., Schwab, Y., and Labouesse, M. (2006). The V0-ATPase mediates apical secretion of exosomes containing Hedgehog-related proteins in Caenorhabditis elegans. J. Cell Biol. *173*, 949–961.

Lu, X., Yu, H., Liu, S.H., Brodsky, F.M., and Peterlin, B.M. (1998). Interactions between HIV1 Nef and vacuolar ATPase facilitate the internalization of CD4. Immunity *8*, 647–656.

Luft, J.H. (1971). Ruthenium red and violet. II. Fine structural localization in animal tissues. Anat. Rec. *171*, 369–415.

Marechal, V., Prevost, M.-C., Petit, C., Perret, E., Heard, J.-M., and Schwartz, O. (2001). Human Immunodeficiency Virus Type 1 Entry

into Macrophages Mediated by Macropinocytosis. J. Virol. *75*, 11166–11177.

Moris, A., Nobile, C., Buseyne, F., Porrot, F., Abastado, J.P., and Schwartz, O. (2004). DC-SIGN promotes exogenous MHC-I-restricted HIV-1 antigen presentation. Blood *103*, 2648–2654.

Morita, E., and Sundquist, W.I. (2004). Retrovirus budding. Annu. Rev. Cell Dev. Biol. *20*, 395–425.

Mujawar, Z., Rose, H., Morrow, M.P., Pushkarsky, T., Dubrovsky, L., Mukhamedova, N., Fu, Y., Dart, A., Orenstein, J.M., Bobryshev, Y.V., et al. (2006). Human immunodeficiency virus impairs reverse cholesterol transport from macrophages. PLoS Biol. *4*, e365. 10.1371/journal.pbio.0040365.

Neil, S.J., Eastman, S.W., Jouvenet, N., and Bieniasz, P.D. (2006). HIV-1 Vpu promotes release and prevents endocytosis of nascent retrovirus particles from the plasma membrane. PLoS Pathog. *2*, e39. 10.1371/journal.ppat.0020039.

Nishi, T., and Forgac, M. (2002). The vacuolar (H+)-ATPases—nature's most versatile proton pumps. Nat. Rev. Mol. Cell Biol. *3*, 94–103.

Nydegger, S., Foti, M., Derdowski, A., Spearman, P., and Thali, M. (2003). HIV-1 egress is gated through late endosomal membranes. Traffic *4*, 902–910.

Nydegger, S., Khurana, S., Krementsov, D.N., Foti, M., and Thali, M. (2006). Mapping of tetraspanin-enriched microdomains that can function as gateways for HIV-1. J. Cell Biol. *173*, 795–807.

Oliveira, H.R., Verlengia, R., Carvalho, C.R., Britto, L.R., Curi, R., and Carpinelli, A.R. (2003). Pancreatic beta-cells express phagocyte-like NAD(P)H oxidase. Diabetes *52*, 1457–1463.

Ongradi, J., Ceccherini-Nelli, L., Pistello, M., Specter, S., and Bendinelli, M. (1990). Acid sensitivity of cell-free and cell-associated HIV-1: Clinical implications. AIDS Res. Hum. Retroviruses *6*, 1433–1436.

Orci, L., Ravazzola, M., Amherdt, M., Madsen, O., Perrelet, A., Vassalli, J.D., and Anderson, R.G. (1986). Conversion of proinsulin to insulin occurs coordinately with acidification of maturing secretory vesicles. J. Cell Biol. *103*, 2273–2281.

Orenstein, J.M., Meltzer, M.S., Phipps, T., and Gendelman, H.E. (1988). Cytoplasmic assembly and accumulation of human immunodeficiency virus types 1 and 2 in recombinant human colony-stimulating factor-1-treated human monocytes: An ultrastructural study. J. Virol. *62*, 2578–2586.

Pelchen-Matthews, A., Kramer, B., and Marsh, M. (2003). Infectious HIV-1 assembles in late endosomes in primary macrophages. J. Cell Biol. *162*, 443–455.

Raposo, G., Moore, M., Innes, D., Leijendekker, R., Leigh-Brown, A., Benaroch, P., and Geuze, H. (2002). Human Macrophages Accumulate HIV-1 Particles in MHC II Compartments. Traffic *3*, 718–729.

Ryzhova, E.V., Vos, R.M., Albright, A.V., Harrist, A.V., Harvey, T., and Gonzalez-Scarano, F. (2006). Annexin 2: A novel human immunodeficiency virus type 1 Gag binding protein involved in replication in monocyte-derived macrophages. J. Virol. *80*, 2694–2704.

Sanfridson, A., Hester, S., and Doyle, C. (1997). Nef proteins encoded by human and simian immunodeficiency viruses induce the accumulation of endosomes and lysosomes in human T cells. Proc. Natl. Acad. Sci. USA *94*, 873–878.

Savina, A., Jancic, C., Hugues, S., Guermonprez, P., Vargas, P., Moura, I.C., Lennon-Dumenil, A.M., Seabra, M.C., Raposo, G., and Amigorena, S. (2006). NOX2 controls phagosomal pH to regulate antigen processing during crosspresentation by dendritic cells. Cell *126*, 205–218.

Sharova, N., Swingler, C., Sharkey, M., and Stevenson, M. (2005). Macrophages archive HIV-1 virions for dissemination in trans. EMBO J. *24*, 2481–2489.

Stumptner-Cuvelette, P., Jouve, M., Helft, J., Dugast, M., Glouzman, A.S., Jooss, K., Raposo, G., and Benaroch, P. (2003). Human immunodeficiency virus-1 Nef expression induces intracellular accumulation of multivesicular bodies and major histocompatibility complex class II complexes: Potential role of phosphatidylinositol 3-kinase. Mol. Biol. Cell *14*, 4857–4870.

Ungermann, C., Wickner, W., and Xu, Z. (1999). Vacuole acidification is required for trans-SNARE pairing, LMA1 release, and homotypic fusion. Proc. Natl. Acad. Sci. USA *96*, 11194–11199.

van Deurs, B., Holm, P.K., and Sandvig, K. (1996). Inhibition of the vacuolar H(+)-ATPase with bafilomycin reduces delivery of internalized molecules from mature multivesicular endosomes to lysosomes in HEp-2 cells. Eur. J. Cell Biol. *69*, 343–350.

van Weert, A.W., Dunn, K.W., Gueze, H.J., Maxfield, F.R., and Stoorvogel, W. (1995). Transport from late endosomes to lysosomes, but not sorting of integral membrane proteins in endosomes, depends on the vacuolar proton pump. J. Cell Biol. *130*, 821–834.

Vergne, I., Chua, J., Singh, S.B., and Deretic, V. (2004). Cell biology of mycobacterium tuberculosis phagosome. Annu. Rev. Cell Dev. Biol. *20*, 367–394.

Welsch, S., Habermann, A., Jager, S., Muller, B., Krijnse-Locker, J., and Krausslich, H.G. (2006). Ultrastructural analysis of ESCRT proteins suggests a role for endosome-associated tubular-vesicular membranes in ESCRT function. Traffic *7*, 1551–1566.

Welsch, S., Keppler, O.T., Habermann, A., Allespach, I., Krijnse-Locker, J., and Krausslich, H.G. (2007). HIV-1 Buds Predominantly at the Plasma Membrane of Primary Human Macrophages. PLoS Pathog. *3*, e36. 10.1371/journal.ppat.0030036.

Yilla, M., Tan, A., Ito, K., Miwa, K., and Ploegh, H.L. (1993). Involvement of the vacuolar H(+)-ATPases in the secretory pathway of HepG2 cells. J. Biol. Chem. *268*, 19092–19100.

Zhen, L., King, A.A., Xiao, Y., Chanock, S.J., Orkin, S.H., and Dinauer, M.C. (1993). Gene targeting of X chromosome-linked chronic granulomatous disease locus in a human myeloid leukemia cell line and rescue by expression of recombinant gp91phox. Proc. Natl. Acad. Sci. USA *90*, 9832–9836.